Use of SF$_6$ to estimate anthropogenic CO$_2$ in the upper ocean

Toste Tanhua,[1] Darryn W. Waugh,[2] and Douglas W. R. Wallace[1]

[1] The highest concentrations of anthropogenic carbon (C_{ant}) are found in the upper layers of the world ocean. However, this is where seasonal variability of inorganic carbon and related parameters due to thermal and biological effects complicates use of back-calculation approaches for C_{ant}. Tracer based approaches to C_{ant} estimation are unaffected by biological variability and have found wide application. However, slow-down, even reversal, of the atmospheric growth of chlorofluorocarbons (CFCs) restricts use of these tracers for C_{ant} estimation for waters ventilated since the mid 1990s. Here we apply SF$_6$, a tracer that continues to increase in the atmosphere, as a basis for the C_{ant} estimation, using samples collected in the midlatitude North Atlantic in 2004. C_{ant} estimates derived from water mass transit time distributions (TTDs) calculated with SF$_6$ are compared to those based on CFC-12. For recently ventilated waters (pCFC-12 > 450 ppt), the uncertainty of SF$_6$ based estimates of C_{ant} is 6 μmol kg^{-1} less than that of CFC-12 based estimates. CFC-12 based estimates remain more reliable for older (deeper) water masses, as a result of the longer input history and more readily detectable concentrations of CFC-12. Historical data suggest that the near-surface saturation of CFC-12 has increased over time, in inverse proportion to its atmospheric growth rate. Use of a time-dependent saturation of CFC-12 in TTD calculations appears to provide more reliable estimation of C_{ant}.

1. Introduction

[2] The World Ocean contains approximately 60 times as much inorganic carbon as the atmosphere, and the anthropogenic perturbation of oceanic dissolved inorganic carbon (DIC) in relation to pre-industrial levels range from approximately 3% (surface waters) to 0% (poorly ventilated deep water). Detection of this small anthropogenic change in DIC against a large and variable natural background represents a formidable analytical and conceptual challenge. A number of inference methods to estimate the oceanic C_{ant} concentration from field data have been developed; including so-called "pre-formed" approaches based on measurements of hydrochemical data such as inorganic carbon, alkalinity, nutrients and oxygen [e.g., *Brewer*, 1978; *Chen and Millero*, 1979; *Gruber et al.*, 1996; *Touratier and Goyet*, 2004; *Friis et al.*, 2005] or, alternatively, tracer-based approaches [e.g., *Thomas and Ittekkot*, 2001; *Hall et al.*, 2002; *Waugh et al.*, 2004]. These different approaches to estimate C_{ant} have various advantages and weaknesses [e.g., *Wallace*, 2001; *Lo Monaco et al.*, 2005; *Matsumoto and Gruber*, 2005; *Tanhua et al.*, 2007; *Vázquez-Rodríguez et al.*, 2008]. Determination of C_{ant} in recently ventilated waters is particularly important

as this is where the highest concentrations of C_{ant} are found. However, it is in the upper water column that the seasonal variability of carbon related hydrochemical parameters arising from thermal and biological effects is the largest.

[3] Several C_{ant} inference methods involve the use of transient tracer data, either to estimate the air-sea disequilibrium for carbon measurement based methods (e.g., the ΔC^* method of *Gruber et al.* [1996]) or as a basis for transfer functions between transient tracers and C_{ant}. The most commonly used transient tracers for C_{ant} inference are chlorofluorocarbons (CFCs; CFC-11 or CFC-12). However, the determination of C_{ant} using CFCs is problematic, especially for recently ventilated waters surveyed after the late 1990s, because the atmospheric concentrations of the CFCs are no longer increasing. The atmospheric concentration of CFC-11 has declined and that of CFC-12 has remained nearly constant since the late 1990s (Figure 1). The decrease in the atmospheric growth rate of CFC-12 is in sharp contrast to the rapidly increasing atmospheric concentration of CO$_2$ (Figure 1, right hand panels) and limits the usefulness of CFC-12 as a proxy for C_{ant}. In contrast, the atmospheric concentration of another tracer, SF$_6$, increases (Figure 1), and an increasing number of ocean measurements of SF$_6$ are becoming available [i.e., *Law and Watson*, 2001; *Watanabe et al.*, 2003; *Vollmer and Weiss*, 2002; *Tanhua et al.*, 2004, 2005; *Bullister et al.*, 2006]. This raises the possibility of using SF$_6$ measurements as a proxy for C_{ant} for recently ventilated waters. The short atmospheric history

---
[1]Leibniz-Institut für Meereswissenschaften, Marine Biogeochemie, Kiel, Germany.
[2]Department of Earth and Planetary Sciences, Johns Hopkins University, Baltimore, Maryland, USA.
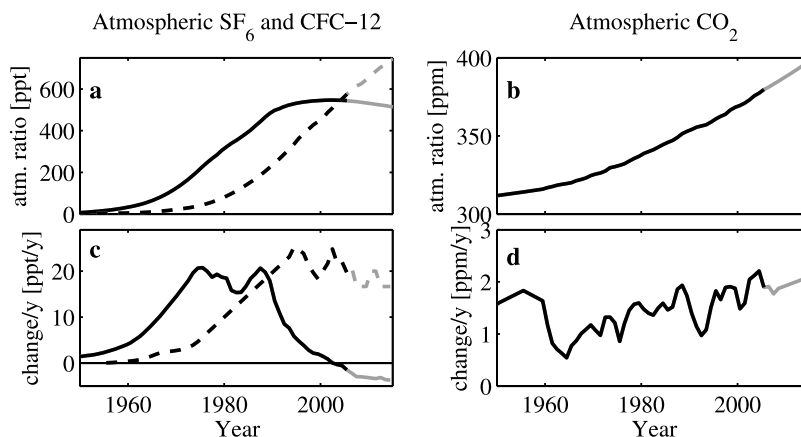
Figure 1. Comparison of atmospheric histories and increase rates of CFC-12, SF$_6$ and CO$_2$. Panel A; the atmospheric mixing ratio of CFC-12 (solid lines) and SF$_6$ *100 (dashed line). Panel C; the growth rate of the two tracers in the atmosphere (SF$_6$*100), the trends are smoothed through a 3-year running mean filter. The atmospheric histories for CFC-12 are from *Walker et al.* [2000] updated from http://gaslab.ucsd.edu/pub/cfchist; for SF$_6$ from *Maiss and Brenninkmeijer* [1998] updated and normalized to data from NOAA/ESRL Global Monitoring Division http://www.cmdl.noaa.gov/infodata/ftpdata.html. Panels B and D shows the atmospheric history and growth rate CO$_2$ (from the Mauna Loa and Law Dome records). The projections for the future (i.e., after year 2006) concentrations and growth rates for CFC-12, SF$_6$ and CO$_2$ used in this study are included in the figures as gray lines.

of SF$_6$ on the other hand makes SF$_6$ less suitable as a proxy for C_{ant} for "older" waters.

[4] In this paper we evaluate the relative magnitudes and sources of uncertainty that influence C_{ant} estimation using CFC-12 and SF$_6$. Specifically, we compare estimates of C_{ant} using the transit time distribution (TTD) approach [*Hall et al.*, 2002] based on measurements of CFC-12 and SF$_6$, and we also compare those measurements with independent estimates calculated with the recently developed eMLR method [*Friis et al.*, 2005; *Tanhua et al.*, 2007].

2. Methods

2.1. Tracer Measurements

[5] The data presented here was collected from the mid-latitude North Atlantic during the spring of 2004 [*Tanhua et al.*, 2006]. The cruise track of Meteor cruise 60 Leg 5 was from Martinique to Lisbon, with a northernmost station at 42°N, and the cruise therefore included sampling of both the subtropical and subpolar gyres, as well as the western and eastern basins (Figure 2). The data are archived at the Carbon Dioxide Information Analysis Center, Oak Ridge National Laboratory, USA, (http://cdiac.esd.ornl.gov/). The anthropogenic carbon content from this data set has been estimated using an empirical approach (C_{ant}^{eMLR}), using measurements made 23 years earlier. The resulting C_{ant} estimates were compared to C_{ant} estimates calculated from TTDs based on CFC-12 data [see *Tanhua et al.*, 2007]. The latter study considered the full water column, but had a special emphasis on the problems of C_{ant} detection in deep and intermediate water masses, in this paper we focus on the upper water column only (0−2000 m).

[6] The determination of SF$_6$ was performed by purge-and-trap gas chromatography with electron capture detection [see *Tanhua et al.*, 2005]. The analytical precision was 1.5%, the detection limit was estimated to be 0.05 fmol kg^{-1} (∼0.15 ppt). A sampling blank (determined from analyses

of deep water samples in the Eastern Basin) of the same magnitude has been subtracted from the data. The SF$_6$ data were calibrated against an air standard prepared at CMDL, Boulder, CO, and are reported on to the GMD2000 scale (http://www.cmdl.noaa.gov/hats/standard/SF6_scale.htm).

[7] The CFC measurements were made on an analytical system similar to that described by *Bullister and Weiss* [1988] and are reported on the SIO98 scale [*Prinn et al.*, 2000]. The analytical precision was 0.7% for CFC-12, and a sampling blank of 0.007 pmol kg^{-1} (determined as the median value of 18 deep water samples in the eastern basin) has been subtracted from the data.

[8] To eliminate the effects of variable temperature and salinity on the tracer solubility, we report tracer concentrations as the equivalent dry air mole fraction for a gas phase in equilibrium with the seawater sample, pCFC or pSF$_6$, i.e.:

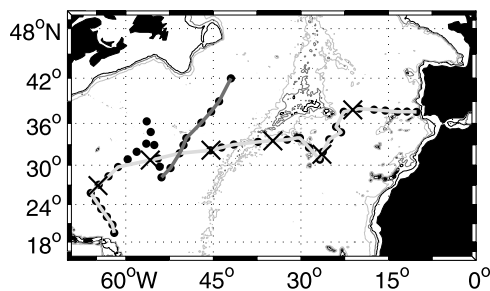$$pCFC = \frac{C_{CFC}}{F(\theta, S)}.$$

Figure 2. Map of the stations occupied during the M60/5 cruise in 2004 (black dots). The light gray line marks the position of the sections shown in Figure 6, where crosses marks every 1000 km distance. The dark gray line marks the sections shown in Figure 7.

[9] The salinity and temperature dependent solubility of the tracers, $F(\theta, S)$, are calculated from their respective solubilities [*Bullister et al.*, 2002; *Warner and Weiss*, 1985], and we have assumed an atmospheric pressure of 1 atmosphere. In this way, tracer concentrations can be compared directly to their time-varying atmospheric histories [*Maiss and Brenninkmeijer*, 1998; *Walker et al.*, 2000] so that "tracer ages" and TTDs of the samples can be determined. We will use the term "tracer age" (τ) for the age derived by simple matching of the tracer concentration (in ppt) to the atmospheric history of the tracer.

2.2. The TTD Method to Determine C_{ant}

[10] In principle, the concentration, c, of a passive tracer in the ocean can be determined at any point, r, and time, t, with knowledge of the transit time distribution, TTD, and the input function of the tracer at the sea-surface, $c_0(t)$, according to

$$c(r,t) = \int_0^\infty c_0(t - t') G(r,t') dt'$$

where $G(r,t)$ is the TTD. To use this equation to calculate C_{ant} it is necessary to know the TTD at each interior ocean location as well as the surface history of C_{ant}. Several different approaches have been used to estimate TTDs. For example, *Thomas et al.* [2001] used TTDs obtained from an ocean circulation model, whereas *Hall et al.* [2002, 2004] and *Waugh et al.* [2004, 2006] estimated TTDs from observations of the concentrations of CFCs and other transient tracers.

[11] Here we use the implementation of *Waugh et al.* [2004, 2006], and we refer the reader to these papers for more details. In this implementation, the TTD at each interior location is assumed to be an inverse Gaussian function [*Waugh et al.*, 2003], with the mean age (Γ) being equal to the width of the TTD (Δ). *Waugh et al.* [2004] demonstrated that TTDs with $\Delta = \Gamma$ is consistent with simultaneous observations of several different transient tracers. With the assumption of a fixed relation between Γ and Δ, the TTD can be defined by the observation of a single transient tracer (e.g., CFC-12 or SF$_6$). The method thus allows for the effects of ocean mixing (Δ) to be considered in establishing the transfer function between the measured tracer concentration and C_{ant}.

[12] The atmospheric history of CO$_2$ is well documented, and by treating concentrations in excess of 280 ppm as the anthropogenic perturbation, C_{ant} can be viewed as a passive transient tracer. The transfer of inorganic carbon from the atmosphere to the ocean is dependent on the buffer-capacity of seawater at the time when the water was in contact with the atmosphere. By using the empirical relations between surface salinity and alkalinity [e.g., *Brewer et al.*, 1986] this can be determined from inorganic carbon chemistry and a knowledge of salinity and temperature alone, and hence the oceanic C_{ant} input function for each water sample can be determined. The TTD of each sample is determined from measurements of transient tracers, and the C_{ant} can then be estimated using the above equation. The TTD method as used here implicitly assumes time-invariable air-sea equi-

librium of CO$_2$, and any temporal changes in the CO$_2$ saturation state will cause systematic biases in the method.

3. Uncertainties in the TTD Method of C_{ant} Estimation

3.1. Sources of Uncertainty and Error

[13] In order to calculate the TTD of a water-sample, the measured tracer concentration has to be compared with the atmospheric history of the tracer. Errors can arise due to: analytical errors in the tracer measurements; uncertainties in the atmospheric history; uncertainties in the Δ/Γ ratio; and uncertainties in the initial degree of saturation of the tracers. We will discuss each of these error sources below.

[14] The uncertainties in the historical atmospheric mixing ratios of the transient tracers CFC-11, CFC-12, CFC-113 and CCl$_4$, as estimated from instrumental records as well as (for earlier periods) industrial production and emission data, are discussed and documented by *Walker et al.* [2000]. For the CFCs these uncertainties are less than 4% for most of the period before reliable atmospheric measurements started, and are considerably less since then. The error in the instrumental record for SF$_6$ atmospheric concentration is also relatively small, (1%) (http://www.cmdl.noaa.gov/infodata/ftpdata.html), but again, uncertainties of atmospheric levels are higher for periods where estimates need to reconstructed based on reported global sales, estimated emissions, atmospheric lifetimes, etc.

[15] The concentration of tracers in seawater can be determined to high accuracy and precision. Realistic numbers for combined calibration and analytical uncertainties are about 2% for CFC-12 and 4% for SF$_6$ [e.g., *Bullister et al.*, 2006; *Tanhua et al.*, 2004]. For samples with low concentrations, the relative error is generally higher so that the error is better represented by an absolute concentration.

[16] A further potential source for bias in SF$_6$ measurements is contamination from any deliberate SF$_6$ injections to the interior of the oceans. These have been conducted since the mid 1980s, and the tracer quantity and position of the releases are well documented [e.g., *Watson and Ledwell*, 2000; *Tanhua et al.*, 2004; *Schmitt et al.*, 2005]. Obviously, care should be taken to avoid influence of any deliberately released SF$_6$ on the C_{ant} calculations. With this problem in mind, a community agreement was reached at the AGU Ocean Science Meeting in 2006 to avoid future use of SF$_6$ in large-scale sub-surface ocean releases.

[17] Most often the surface tracer concentration is not fully in equilibrium with the atmosphere, particularly during winter time convection. Hence further uncertainty arises from the need to assume or estimate a degree of air-water equilibration (saturation) for the tracer at the time of water mass formation. This uncertainty in the assumed saturation is usually larger than the analytical error. It is known that the depth of the seasonal mixed layer as well as the rate of atmospheric increase influence the surface saturation of the tracers [e.g., *Haine and Richards*, 1995]. For instance, water masses that are formed during very deep convection have been reported to have CFC saturations as low as 60% [*Wallace and Lazier*, 1988]. Similarly, *DeGrandpre et al.* [2006] found under-saturated conditions in the Labrador Sea through the whole year with respect to CO$_2$. Comparing
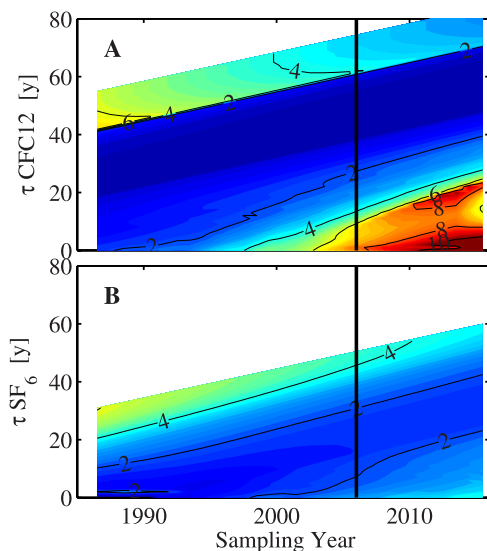
Figure 3. Errors in C_{ant} calculations using the TTD method (in μmol kg^{-1}). For these calculations, we have assumed 6% error in correctly assuming the saturation of the tracer and an analytical error of 4% or 0.1 ppt for SF_6 and 2% or 5 ppt for CFC-12, whichever of these two errors are the largest. These errors are color-contoured as a function of sampling year and tracer age (τ) for the respective tracer. Panel A; calculated with CFC-12 data; and Panel B with SF_6 data. The areas to the right of the black line are future projections of the error assuming a trend for the tracers as in Figure 1, as well as exponentially increasing C_{ant} concentration.

CFC measurements from the ocean interior with data simulated in an advection-diffusion model, *Mecking et al.* [2004] estimated initial saturations of CFC-12 ranging from 80–100%, with the initial saturation being correlated with density. Similarly, by comparing the saturation of all surface water samples from a cruise in the Southern Ocean, *Tanhua et al.* [2004] found uncertainties in saturation of ~5%. The combined error in determination of the tracer equilibrium concentration can thus be in the order of 10%, or larger for lower concentration samples. These errors will lead to errors in estimated C_{ant}, particularly for time periods when the tracer concentration in the atmosphere has increased slowly (see below).

[18] The TTD-method is dependent on an assumed shape for the TTD. In the case of the inverse Gaussian distribution that has been assumed here, the relation between the mean age and the width of the TTD, i.e., the Δ/Γ ratio, is critical. The effect of varying this ratio on C_{ant} estimation has been demonstrated by *Waugh et al.* [2004], Figure 7. Although there are large differences in C_{ant} for Δ/Γ ratio that vary from 0 to 1 (i.e., between a "no mixing" case and "more realistic" mixing), the difference between, for instance, ratios of 1.25 or 0.75 versus unity are relatively small (on the order of 1 μmol kg^{-1}).

[19] There are additional sources of uncertainty in the TTD approach to C_{ant} estimation, including not accounting for possible anthropogenic effects on the biological or physical transport of carbon within the ocean interior, and

the assumption of time-independent air-sea disequilibrium for CO_2. Even though the saturation of C_{ant} and CFC tracers have fundamentally different response to changes in temperature [*Thomas and England*, 2002], a general warming (or cooling) of the oceans will not directly influence C_{ant} estimates using the TTD method since temperature is accounted for. A potentially significant error could be introduced by changes in the air-sea equilibrium of CO_2 and tracers (a method allowing for time-variant air-sea disequilibrium of CO_2 is demonstrated by *Hall et al.* [2004]). These uncertainties apply equally to the C_{ant} estimates independent of the tracer (e.g., SF_6 or CFC-12) used to calculate the TTD, and are not discussed further here.

3.2. Time and Age-Dependence of Uncertainties

[20] Due to variability in historical atmospheric growth rates, the magnitude of errors associated with most of the sources of uncertainty listed above will differ depending on which tracer is used (e.g., SF_6 or CFC-12). Errors will also vary with the "age" of the water mass, and the time of sampling. The uncertainties in C_{ant} estimates for the two tracers are plotted as a function of tracer age and year of sampling in Figure 3. The plot is based on an assumed 6% uncertainty in the saturation of the tracer. The analytical uncertainties is assumed to be 4% or 0.1 ppt for SF_6 and 2% or 5 ppt for CFC-12 (whichever of the absolute or percentage error is the largest).

[21] For this analysis we have also included uncertainty in the atmospheric history as given by *Walker et al.* [2000] for CFC-12, and an assumed error for SF_6 of 0.005 ppt. We applied projections for the atmospheric concentrations of CO_2 and the tracers as shown in Figure 1 in order to assess possibly future uncertainties.

[22] Figure 3, top panel, shows that errors in C_{ant} calculated from TTDs based on CFC-12 (C_{ant}^{F12}) are high for "young" samples that have been sampled recently (or will be sampled in the future). This is due to the reduced (or negative) atmospheric growth rate of CFC-12 since the mid 1990s. There is also a band of larger errors for the "oldest" measurable tracer ages. These errors mainly arise from analytical uncertainty, in this case assumed to be 5 ppt which corresponds to a blank of roughly 0.03 pmol kg^{-1}. This may be a worst-case scenario.

[23] The situation for the error in C_{ant} calculated with TTDs based on SF_6 (C_{ant}^{SF6}) is different (Figure 3, lower panel), with relatively low errors for "younger" waters but with analytical errors being more significant for "older" samples due to lower concentrations and lower analytical precision for SF_6 compared to CFC-12. The reason for the absence of a band of high errors for old samples is due to the different way in which we have treated very low SF_6 concentrations: for CFC-12 it is often assumed (also for our analysis) that zero CFC-12 concentration equals zero C_{ant}, whereas for SF_6 we assigned samples with zero SF_6 concentration to "not available". The reason for the different treatment is the significantly different length of the atmospheric histories of the two tracers. However, since the anthropogenic emissions of CO_2 started over 150 years before emissions of CFC-12, C_{ant} can potentially be present also in CFC-12 samples below the detection limit. In fact, the surface ocean imprint of C_{ant} around 1940 (i.e., before

Table 1. List of Cruises From the Preliminary Release of the CARINA Database That Have Been Used for Our Analysis of Historical Saturation of CFC-12, See http://cdiac.ornl.gov/oceans/CARINA/Carina_inv.html; Carbon Dioxide[a]

Expocode	Chief Scientist	CFC PI
34AR19970805	H. Gronvall & J. Launiainen	T. Tanhua
74DI19970807	A. F. Rios	D. Smythe-Wright
32EV19910529	?	?
58GS20030922	T. Johannessen	K.A. Olsson & E. Jeansson
18HU19820228	R. Clarke, JL Reid, J Swift	R. Weiss & D. Wallace
18HU19920527	J. Lazier	P. Jones
18HU19930617	J. Lazier	P. Jones
18HU19931115	A. Clarke	P. Jones
18HU19940524	J. Lazier	P. Jones
18HU19941012	A. Clarke	P. Jones
18HU19970509	A. Clarke	P.Jones & R. Gershey
58JH19911106	J. Blindheim	J. Bullister
58JH19931107	J. Blindheim & F.Rey	J. Bullister
58JH19940723	J. Blindheim	E. Fogelqvist & T.Tanhua
58JH19941029	J. Blindheim & F. Rey	J. Bullister
58JH19951108	F. Rey	J. Bullister
58JH19961030	J. Blindheim & F. Rey	J. Bullister
58JH19970425	J. Blindheim & F. Rey	J. Bullister
58JH19990616	J. Blindheim & F. Rey	J. Bullister
06MT19941012	P. Koltermann & J. Meincke	W. Roether
06MT19941115	J. Meincke	W. Roether & M. Rhein
06MT19970517	W. Zenk & T. Mueller	O. Plöhn
06MT19970707	F. Schott	M. Rhein
06MT20040311	D. Wallace	T. Tanhua

[a]Information Analysis Center, Oak Ridge National Laboratory, US Department of Energy, Oak Ridge, Tennessee, for data and more details. The year of sampling can be as characters 5–8 in the expocode.

the use of CFCs) was in excess of 10 μmol kg^{-1}. However, applying the TTD method to contemporary CFC data with a detection limit of 0.005 pmol kg^{-1}, this error will only be about 2 μmol kg^{-1} C_{ant}, due to the effects of mixing.

[24] The uncertainty in the atmospheric history is of second order importance in comparison to analytical errors for the low concentration range of both tracers. For the recently ventilated samples, the estimate is dependent more on atmospheric history as determined by instrumental measured records of CFC-12/SF$_6$, and these are very accurate (see above).

4. Results From the North Atlantic

4.1. Initial Saturation of the Tracers

[25] We start our analysis with the uncertainty in C_{ant} associated with uncertainty in the initial surface saturation of the tracer. During the M60/5 cruise, the average surface saturation for CFC-12 was 100% (standard deviation 3.8%), whereas for SF$_6$ it was only 88% (standard deviation 7.5%). The difference is possibly associated with the difference in the contemporary atmospheric growth rates of the two tracers. To test this hypothesis we analyzed the mean saturation of CFC-12 for all the North Atlantic cruises in the GLODAP database [*Key et al.*, 2004] as well as a preliminary version of the CARINA database (see Table 1 for details). Even though the data were collected from cruises from various regions of the North Atlantic (including the Nordic Seas and the Labrador Sea), and were sampled during various seasons, there is a tendency for CFC-12 to have been under-saturated during earlier cruises, and to be close to saturation for later cruises (Figure 4a). In fact, a 2nd order polynomial fit to the data resembles the shape of the atmospheric concentration over time for

CFC-12 with a time-lag of ~5 years (Figure 1a). To test this we plotted the best fit of the CFC-12 saturation from Figure 4a versus the atmospheric growth rate of CFC-12 (Figure 1c) in Figure 4b.

[26] The apparent inverse correlation between atmospheric growth rate and surface saturation for CFC-12 is presumable typical for other CFCs and SF$_6$ as well. Typical gas-exchange velocities can equilibrate shallow surface mixed layers with the atmosphere on timescales of weeks to months. In comparison, atmospheric growth (e-folding) timescales for these compounds were never less than several years which implies that the rate of gas transfer into shallow mixed layers is not the reason for this inverse correlation. The correlation is more likely associated with temporal trends in subsurface vertical gradients of the tracers in the context of deep mixing and/or mixing with sub-surface water. Specifically, it implies that the subsurface gradients of CFC-12 have become less steep as its atmospheric growth rates has decreased. In a deep-mixing scenario, this implies less dilution of surface CFC-12 levels by sub-surface waters entrained during convection. In an upwelling scenario, the surface layer CFC-12 is diluted to a lesser extent by upwelled water.

[27] Figure 1 shows that the SF$_6$ atmospheric growth rate has remained relatively constant over the last ~20 years whereas the CFC-12 growth rate has decreased steadily over the same time period; this implies that SF$_6$ surface saturations are likely to have remained more constant than CFC-12 saturations over the same period. We therefore calculated TTDs with SF$_6$ data from M60/5 for a time-invariant surface saturation of 86%. Note that this value is very similar to the best fit CFC-12 saturation around 1990 at a time when the CFC-12 atmospheric growth rate was similar to the present-day SF$_6$ atmospheric growth rate. The TTDs based on SF$_6$
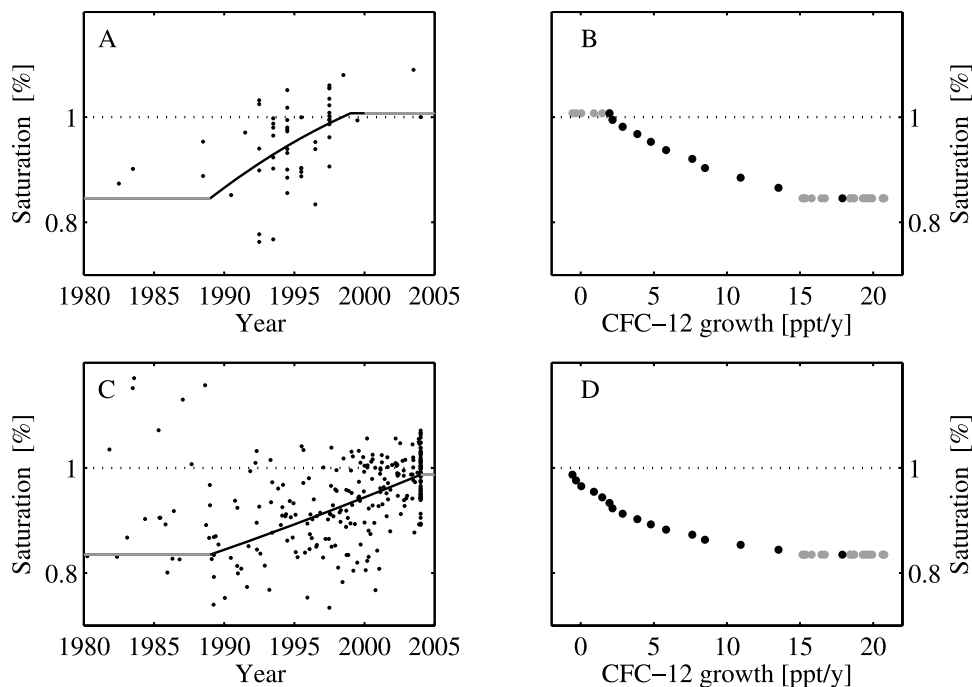
Figure 4. Panel A: The per cruise mean saturation of CFC-12 from each of the North Atlantic cruises in the GLODAP [*Key et al.*, 2004] and a preliminary version of the CARINA (http://cdiac.ornl.gov/oceans/ CARINA/Carina_inv.html, Table 1) databases. The combined data set consists of 57 independent cruises with CFC-12 data to the North Atlantic. The black line is a 2nd order polynomial fit to the data between 1985 and 2000, constant saturation is assumed before and after these times (gray line). Panel B: The CFC-12 saturation as determined from the fit in panel A plotted versus the atmospheric annual growth rate of CFC-12 (Figure 1c) as black dots (gray dots for the time outside of the fit, where the saturation is set). Panel C: The SF$_6$ ventilation year in each data point from the M60/5 cruise, assuming 86% saturation versus the saturation of CFC-12 determined by the best fit with the SF$_6$ mean ages. Panel D: The CFC-12 saturation as determined from the fit in panel C plotted versus the atmospheric annual growth rate of CFC-12 (Figure 1c) as black dots (gray dots for the time outside of the fit, where the saturation is set).

data were used to predict CFC-12 concentrations for the same water samples based on an assumption of time-invariant 100% initial saturation, and the predicted CFC-12 concentrations were compared to measured values. Figure 4c shows the corresponding ratios of measured/predicted CFC-12 versus the mean age of the water sample, and this ratio is also plotted versus the atmospheric growth rate in Figure 4d. If the SF$_6$ based TTDs are accurate, then the measured/ predicted ratio of CFC-12 is an indication of the initial surface saturation of CFC-12.

[28] These two lines of evidence, i.e., the historical CFC-12 data and the comparison of SF$_6$ and CFC-12 data from the M60/5 cruise, suggest that the surface saturation of these tracers are inversely correlated with the atmospheric growth rate. Time-dependent saturation of CFC-12 and CFC-11 has been observed in the Labrador Sea [*Azetsu-Scott et al.*, 2003, 2005], where the variations in saturation were correlated to different convection regimes in the Labrador Sea. A similar time-dependence for the saturation of CFC-11 was found by *Zhao et al.* [2006, Figure 13] for the Labrador Sea from an ocean circulation model.

[29] Hence for the calculations below we have assumed a time-varying saturation of CFC-12 which follows the solid line shown in Figure 4a, where the saturation for recent samples is set to 100% and for older samples to 86%. There are too few data to constrain the surface saturation with growth rate further back in time. We also use a time-invariant saturation of 86% for SF$_6$ since this is close to the measured saturation during 2004 and because the contemporary atmospheric growth rate of SF$_6$ is similar to that of CFC-12 during the 1970s and 1980s. The assumed constant saturation of SF$_6$ regardless of tracer age, is necessary due to a lack of historic data and justified by the almost linear increase of SF$_6$ since about 1990. The influence of other, potentially important, factors including temporal variation in the depth of convection is not considered. However, as we will see below, even such a simple treatment of time-variable saturation improves the agreement between C_{ant} estimates calculated using CFC-12 and SF$_6$.

4.2. Distribution of Tracers and C$_{ant}$

[30] The TTD method as described above was used to estimate C_{ant} from SF$_6$ and CFC-12 measurements from the 2004 North Atlantic cruise M60/5. In the C_{ant} calculations shown below we use $\Delta/\Gamma = 1$ and the above-described treatment of initial saturations of the tracers. Inevitable some samples will be "supersaturated" (i.e., will have a
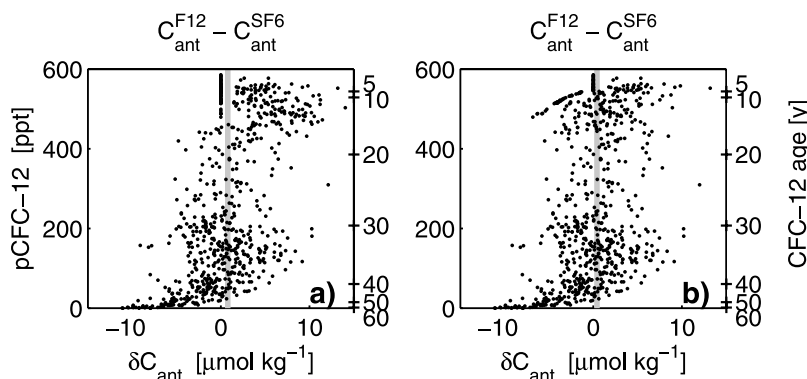
Figure 5. Difference in anthropogenic carbon content from the M60/5 cruise calculated using the TTD method, based either on SF$_6$ or CFC-12 measurements, plotted versus pCFC-12. The gray lines mark the mean difference in the range 100 to 450 ppt CFC-12. The right hand scale of the panels shows the CFC-12 tracer age (τ) corresponding to the pCFC-12 on the left hand scale. In panel A we have assumed a constant saturation of 86% for both tracers, whereas in panel B we have assumed a time-dependent saturation for CFC-12 (the line in Figure 4a), and 86% saturation for SF$_6$.

saturation in excess of 86% for SF$_6$, resulting in "negative ages"), primarily close to the surface. Samples with dry air mole fraction equivalent for the tracer that are in excess of contemporary values were therefore set to be "recent" (i.e., age = 0 y) and the C_{ant} concentration was calculated from the contemporary atmospheric pCO$_2$ of 2004.

[31] Figure 5 compares estimates of C_{ant} calculated from the SF$_6$ (C_{ant}^{SF6}) and CFC-12 (C_{ant}^{F12}) measurements. Panel (a) shows results calculated for the time-invariant saturation for both tracers of 86%, whereas panel (b) presents results calculated with the time-dependent surface saturation of CFC-12. The difference between the C_{ant}^{F12} and C_{ant}^{SF6} tends to zero in the surface waters because our approach forces
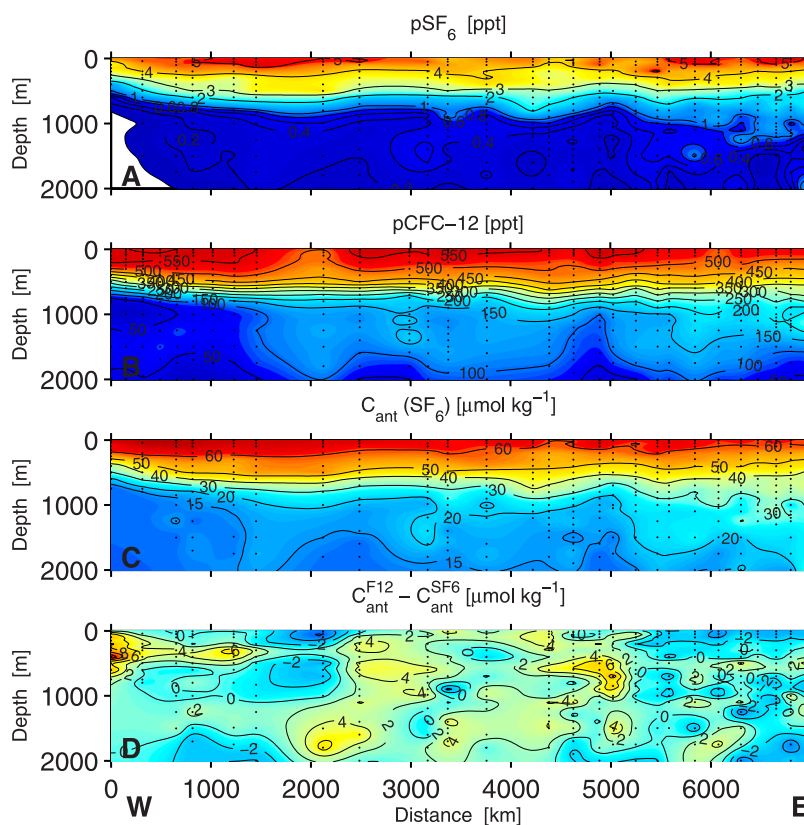

Figure 6. West-east sections of the top 2000 m depth across the midlatitude North Atlantic (Figure 2, light gray line). Panel A shows the measured pSF$_6$ concentration [ppt]; Panel B the measured pCFC-12 concentration [ppt]; Panel C the C_{ant}^{SF6} concentration [μmol kg^{-1}]; Panel D shows the difference $C_{ant}^{F12} - C_{ant}^{SF6}$ [μmol kg^{-1}].
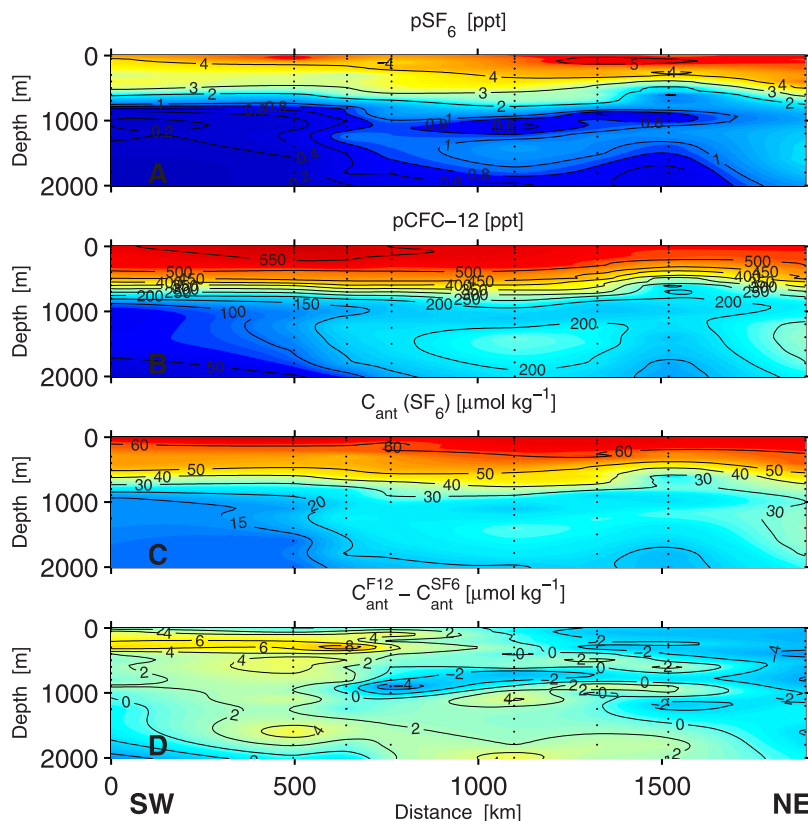
Figure 7. South-north sections of the top 2000 meters depth across the midlatitude North Atlantic (Figure 2, dark gray line). Panel A shows the measured pSF$_6$ concentration [ppt]; Panel B the measured pCFC-12 concentration [ppt]; Panel C the C_{ant}^{SF6} concentration [μmol kg^{-1}]; Panel D shows the difference $C_{ant}^{F12} - C_{ant}^{SF6}$ [μmol kg^{-1}].

"supersaturated" samples to have C_{ant} values that are in equilibrium with contemporary atmospheric pCO$_2$. For samples with pCFC-12 > 450 ppt, C_{ant}^{F12} is generally greater than C_{ant}^{SF6}, particularly for the time-invariant initial saturation case (panel a). The tendency for C_{ant}^{F12} to be greater than C_{ant}^{SF6} for high pCFC-12 samples is significantly reduced when the time-dependent initial saturation of CFC-12 is considered (panel b). For samples with pCFC-12 values between 100 and 450 ppt, there is generally good agreement between C_{ant}^{F12} and C_{ant}^{SF6}, with the mean difference being 0.8 ± 3.4 and 0.4 ± 3.4 μmol kg^{-1} for cases a) and b), respectively. The depth of the upper horizon where the two estimates agree closely (i.e., the pCFC-12 = 450 ppt isoline) is dependent on the local hydrography and corresponds to C_{ant} concentrations of about 40 μmol kg^{-1} in 2004. For older samples, i.e., samples with pCFC-12 < 100 ppt, C_{ant}^{SF6} is generally higher than C_{ant}^{F12}. The reason for this is two-fold; measurement uncertainties associated with very low pSF$_6$ values; as well as the short atmospheric history of SF$_6$. The difference between the C_{ant} history and SF$_6$ history is larger than that between C_{ant} and CFC-12, making SF$_6$ a poor proxy for C_{ant} in older waters.

[32] Figures 6 and 7 shows sections of pSF$_6$, pCFC-12, C_{ant}^{SF6}, and the difference between the two C_{ant} estimates ($C_{ant}^{F12} - C_{ant}^{SF6}$), using the time-dependent initial saturation for CFC-12. As discussed above there is generally good agreement between the two estimates in the surface and below about 800 m, but there are larger differences in a subsurface layer. For the western basin C_{ant}^{F12} is up to 10 μmol kg^{-1} higher than C_{ant}^{SF6} in a subsurface layer between 200-500 m depth. However, for the Eastern Basin and in the northern part of section 2, the two C_{ant} estimates are more consistent. The column inventory based on CFC-12 data for the upper 800 m during the M60/5 cruise is generally larger than the SF$_6$ based inventory (average ~1 mol m^{-2}), although at individual stations this difference can be as large as 6 mol m^{-2}, i.e., up to roughly 6% of the total column inventory. The exception is the northernmost station (at 42°N) where the SF$_6$ based column inventory is larger by about 3 mol m^{-2} (Figure 7d).

4.3. Uncertainty Arising From the Δ/Γ Ratio

[33] We now explore the uncertainty associated with assuming a Δ/Γ ratio of 1 in the TTD calculations. We first compare the measured pSF$_6$ versus pCFC-12 from the M60/5 cruise in Figure 8. The dashed-dotted gray line is the SF$_6$/CFC-12 relation of the atmospheric history of these tracers, with selected time-markers indicated. All data points from the ocean would fall on this line in the extreme case of no mixing of waters with different ages (i.e., if Δ/Γ = 0). Clearly, the observations fall closer to a line that can be represented by assuming strong mixing within the ocean (i.e., Δ/Γ = 1), which is an indication that this ratio of mean age over the width of the TTD is realistic. The atmospheric histories of the two tracers are however not sufficiently different to allow exclusion of even stronger
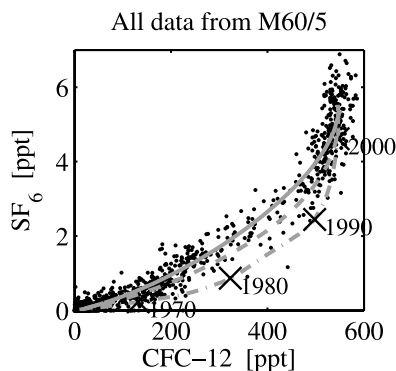
Figure 8. The dry air mole fraction of SF$_6$ versus the dry air mole fraction of CFC-12 for the M60/5 data set from year 2004 plotted as black dots. The gray dash-doted line is the atmospheric concentration of the two tracers over time, where a cross marks every 10-year. This line is equal to the expected relation between the two tracers in the ocean with assumption of no mixing ($\Delta/\Gamma = 0$), the dashed line is the oceanic relation if $\Delta/\Gamma = 0.5$ (i.e., moderate mixing) and the solid line is for the $\Delta/\Gamma = 1$ (i.e., strong mixing) case. For this plot we have assumed time-dependent saturation of CFC-12, and constant 86% saturation of SF$_6$.

mixing, although a ratio of $\Delta/\Gamma = 1$ was shown by *Waugh et al.* [2004] to be consistent with relations between several tracers.

[34] The dependence of the calculated TTDs to variation of the assumed Δ/Γ ratio is different for SF$_6$ and CFC-12, and this translates into differences in the resulting C_{ant} estimates. Figure 9 shows the difference in C_{ant} estimates based on SF$_6$ and CFC-12 for different assumed values of the Δ/Γ ratio. The gray lines in the panels indicate the averaged difference in the tracer age interval for which there is good agreement between SF$_6$ and CFC-12 based C_{ant} estimates. The difference in C_{ant} is generally relatively small for the three cases, indicating that the sensitivity to the Δ/Γ ratio for the C_{ant} calculation is relatively small. The good fit for estimates based on Δ/Γ ratio of 1 is another indication that this indeed might be a reasonable approximation of ocean mixing.

4.4. Comparison to eMLR Based Estimates

[35] The so-called "extended Multiple Linear Regression" (eMLR) method for C_{ant} estimates of *Friis et al.* [2005] uses multiple linear regressions of dissolved inorganic carbon on repeated measurements of inorganic carbon and related hydrochemical properties. The coefficients of the two regressions are subtracted resulting in a new multivariate equation that predicts the differences in DIC between the two data sets that are not correlated with temporal changes of the underlying hydrochemical parameters. The interpretation is that natural variability of DIC between the two dats sets are compensated via the regression on hydrochemical parameters that are known to influence DIC (e.g., oxygen and temperature changes) whereas the remaining "unexplained" differences relate to changes in C_{ant} (ΔC_{ant}) between the two surveys. The total C_{ant} can then be estimated from ΔC_{ant} via an extrapolation method

presented by *Tanhua et al.* [2007]. More information on the approach as well as a comparison between the TTD method (CFC-12) and the eMLR method using the same data set but focusing more on deeper layers are presented by *Tanhua et al.* [2007]. Importantly, the resulting estimates from the eMLR method are completely independent of transient tracer data.

[36] This comparison reveals larger differences of C_{ant} estimates between the two methods (eMLR versus TTD) than between the TTD method using the two tracers. Figure 10a show the difference between the eMLR and TTD derived estimates of C_{ant}, and Panels B and C show box and whisker plots for all samples from M60/5. It is notable that there are a number of shallow samples for which there are large (~20 umol kg^{-1}) discrepancies between the TTD and eMLR based methods, and that the spread of C_{ant} estimates for the shallower samples is smaller for the TTD method (panel B), than for the eMLR method (panel C). This is most likely due to seasonal variations in carbon related properties such as oxygen, nutrients and DIC. These variations can affect estimates of C_{ant} from the eMLR method, but are not directly effecting the TTD method. The spread and the absolute values of the two C_{ant} estimates are quite similar for deeper samples. It seems that the tracer-based TTD method may be preferable to the eMLR method
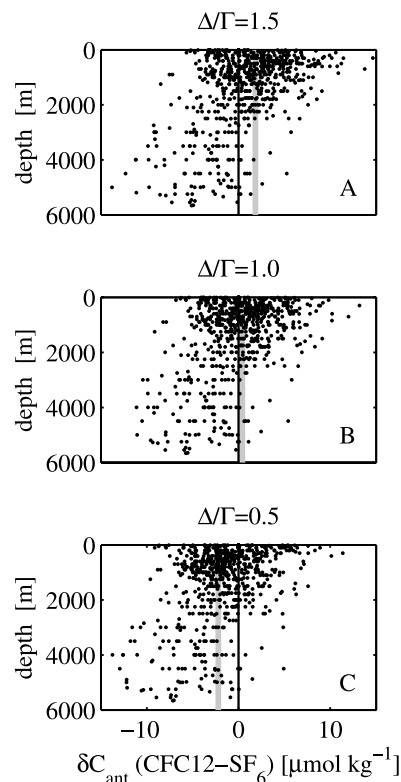

Figure 9. Difference in anthropogenic carbon content based either on SF$_6$ or CFC-12 measurements (calculated using the TTD method) plotted versus depth for different assumptions on mixing. The data are from the M60/5 cruise in 2004. The gray lines mark the mean difference in the CFC-12 concentration range of 100 to 450 ppt (see Figure 5). Panel A assumes a Δ/Γ ratio of 1.5; panel B 1.0; and panel C 0.5.
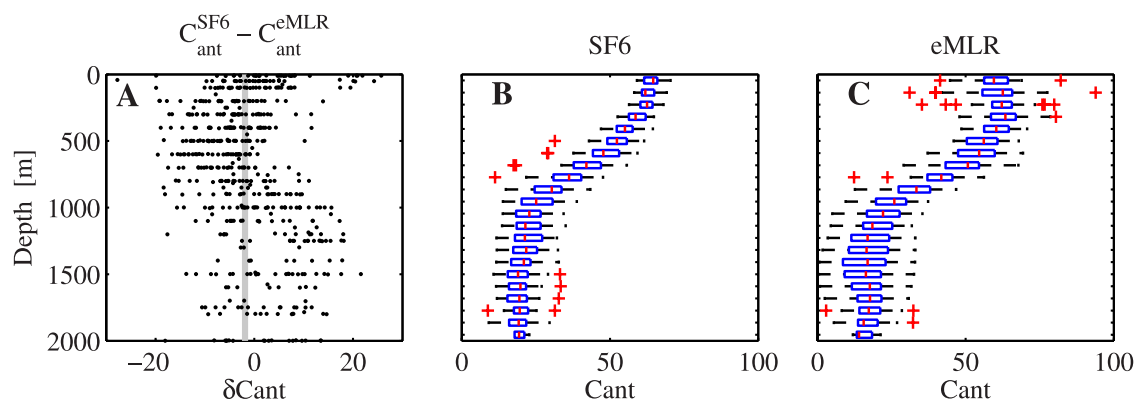
Figure 10. Comparison of C_{ant} estimates using either the TTD method applied on SF$_6$ data or the eMLR method. Panel A: The difference between C_{ant}^{SF6} and C_{ant}^{eMLR} (μmol kg^{-1}) versus depth for all the data from the M60/5 cruise above 2000 m. Note the larger scale for the x axis compared to Figures 5 and 9. Panels B and C are box and whisker plots of C_{ant}^{SF6} and C_{ant}^{eMLR}, respectively, where the C_{ant} concentrations (in μmol kg^{-1}) are interpolated to standard depths (10 50 100:100:2000 m depth). Each box defines the lower and upper quartile of the data, the whiskers shows the extent of the rest of the data, with outliers marked with red crosses.

in the upper part of the ocean that is strongly affected by seasonal variations.

5. Conclusion

[37] SF$_6$ and CFC-12 based estimates of C_{ant} using the TTD method have different sensitivities to uncertainties in the measurement of the tracer and to assumptions regarding the initial saturation of the tracer at the time of water mass formation. We have shown that the post-1980s reduction of the atmospheric growth rate of CFC-12 increases the uncertainty of C_{ant} estimations based on CFC-12 for samples ventilated recently, although the effect on older waters is small. For data collected before the end of the 1990s (e.g., WOCE data and the GLODAP synthesis), the CFC-12 growth rate was still sufficiently high to allow accurate determination of TTDs, and thus C_{ant}. However, for more recent data, i.e., for pCFC-12 > 450 ppt, the uncertainty associated with the TTD estimation is rapidly increasing.

[38] We have demonstrated an empirical relationship between atmospheric growth rate of CFC-12 and its mean surface saturation. Applying this time-dependency in the TTD calculation improves the agreement between SF$_6$ and CFC-12 based estimates of C_{ant}.

[39] Data from a cruise in the midlatitude North Atlantic show generally positive values of C_{ant}^{F12}-C_{ant}^{SF6} for recently ventilated samples, i.e., samples with higher C_{ant} concentrations. This is most likely due to errors in the assumption of initial saturation, which will affect C_{ant}^{F12} estimates considerable more than C_{ant}^{SF6} estimates, Figure 3. As C_{ant}^{SF6} is less sensitive to uncertainties in the assumed initial saturation, this estimate is likely a better basis for C_{ant} estimation in the upper water column. For older samples, i.e., with pCFC-12 < 100 ppt, C_{ant}^{SF6} is systematically higher than C_{ant}^{F12}. This likely relates to difficulties associated with making accurate measurements of very low SF$_6$ concentrations in the deep ocean, as well as a larger difference between the C_{ant} and SF$_6$ histories than between the C_{ant} and CFC-12 histories.

[40] Since the CFC-12 can to date be determined with higher precision and accuracy, it tends to produce more precise C_{ant} estimates for samples with pCFC < 450 ppt. As the atmospheric concentration of CFC-12 is now decreasing, and is predicted to continue to do so, we have demonstrated that CFC measurements benefit from complementary SF$_6$ measurements, and that the SF$_6$ data provide a better basis for tracer based C_{ant} estimations in recently ventilated waters.

References

Azetsu-Scott, K., E. P. Jones, I. Yashayaev, and R. M. Gershey (2003), Time series study of CFC concentrations in the Labrador Sea during deep and shallow convection regimes (1991–2000), *J. Geophys. Res.*, *108*(C11), 3354, doi:10.1029/2002JC001317.

Azetsu-Scott, K., E. P. Jones, and R. M. Gershey (2005), Distribution and ventilation of water masses in the Labrador Sea inferred from CFCs and carbon tetrachloride, *Mar. Chem.*, *94*, 55–66, doi:10.1016/j.marchem. 2004.07.015.

Brewer, P. G. (1978), Direct observation of the oceanic CO2 increase, *Geophys. Res. Lett.*, *5*(12), 991–1000.

Brewer, P., A. L. Bradshaw, and R. T. Williams (1986), Measurements of total carbon dioxide and alkalinity in the North Atlantic Ocean in 1981, in *The Changing Carbon Cycle. A Global Analysis*, edited by J. R. Trabalka and D. E. Reichele, Springer-Verlag, New York.

Bullister, J. L., and R. F. Weiss (1988), Determination of CCl$_3$F and CCl$_2$F$_2$ in seawater and air, *Deep Sea Res.*, *35*, 839–853.

Bullister, J. L., D. P. Wisegarver, and F. A. Menzia (2002), The solubility of sulfur hexafluoride in water and seawater, *DeepSea Res., Part I*, *49*, 175–187.

Bullister, J. L., D. P. Wisegarver, and R. E. Sonnerup (2006), Sulfur hexa-fluoride as a transient tracer in the North Pacific Ocean, *Geophys. Res. Lett.*, *33*, L18603, doi:10.1029/2006GL026514.

Chen, C.-T., and F. Millero (1979), Gradual increase of oceanic CO2, *Nature*, *277*, 1093.

DeGrandpre, M. D., A. Kortzinger, U. Send, D. W. R. Wallace, and R. G. J. Bellerby (2006), Uptake and sequestration of atmospheric CO2 in the Labrador Sea deep convection region, *Geophys. Res. Lett.*, *33*, L21503, doi:10.1029/2006GL026881.

Friis, K., A. Körtzinger, J. Pätsch, and D. W. R. Wallace (2005), On the temporal increase of anthropogenic CO₂ in the subpolar North Atlantic, *DeepSea Res., Part I*, *52*, 681–698, doi:10.1016/j.dsr.2004.11.017.

Gruber, N., J. L. Sarmiento, and T. F. Stocker (1996), An improved method for detecting anthropogenic CO2 in the oceans, *Global Biogeochem. Cycles*, *10*(4), 809–837.

Haine, T. W. N., and K. J. Richards (1995), The influence of the seasonal mixed layer on oceanic uptake of CFCs, *J. Geophys. Res.*, *100*(C6), 10,727–10,744.

Hall, T. M., T. W. N. Haine, and D. W. Waugh (2002), Inferring the concentration of anthropogenic carbon in the ocean from tracers, *Global Biogeochem. Cycles*, *16*(4), 1131, doi:10.1029/2001GB001835.

Hall, T. M., D. W. Waugh, T. W. N. Haine, P. E. Robbins, and S. Khatiwala (2004), Estimates of anthropogenic carbon in the Indian Ocean with allowance for mixing and time-varying air-sea CO2 disequilibrium, *Global Biogeochem. Cycles*, *18*, GB1031, doi:10.1029/2003GB002120.

Key, R. M., A. Kozyr, C. L. Sabine, K. Lee, R. Wanninkhof, J. L. Bullister, R. A. Feely, F. J. Millero, C. Mordy, and T. H. Peng (2004), A global ocean carbon climatology: Results from Global Data Analysis Project (GLODAP), *Global Biogeochem. Cycles*, *18*, GB4031, doi:10.1029/2004GB002247.

Law, C. S., and A. J. Watson (2001), Determination of Persian Gulf water transport and oxygen utilisation rates using SF₆ as a novel transient tracer, *Geophys. Res. Lett.*, *28*(5), 815–818.

Lo Monaco, C., C. Goyet, N. Metzl, A. Poisson, and F. Tourtier (2005), Distribution and inventory of anthropogenic CO2 in the southern ocean: Comparison of three data-based methods, *J. Geophys. Res.*, *110*, C09502, doi:10.1029/2004JC002571.

Maiss, M., and C. A. M. Brenninkmeijer (1998), Atmospheric SF6: Trends, sources, and prospects, *Environ. Sci. Technol.*, *32*, 3077–3086.

Matsumoto, K., and N. Gruber (2005), How accurate is the estimation of anthropogenic carbon in the ocean? An evaluation of the DeltaCstar method, *Global Biogeochem. Cycles*, *19*, GB3014, doi:10.1029/2004GB002397.

Mecking, S., M. J. Warner, C. E. Greene, S. L. Hautala, and R. E. Sonnerup (2004), Influence of mixing on CFC uptake and CFC ages in the North Pacific thermocline, *J. Geophys. Res.*, *109*, CO7014, doi:10.1029/2003JC001988.

Prinn, R. G., et al. (2000), A history of chemically and radiatively important gases in air deduced from ALE/GAGE/AGAGE, *J. Geophys. Res.*, *105*, 17,751–17,792, doi:10.1029/2006GB002695.

Schmitt, R. W., J. R. Ledwell, E. T. Montgomery, K. L. Polzin, and J. M. Toole (2005), Enhanced diapycnal mixing by salt fingers in the thermocline of the Tropical Atlantic, *Science*, *308*, 685–688.

Tanhua, T., K. A. Olsson, and E. Fogelqvist (2004), A first study of SF₆ as a transient tracer in the southern ocean, *Deep Sea Res., Part II*, *51*, 2683–2699.

Tanhua, T., K. Bulsiewicz, and M. Rhein (2005), Spreading of overflow water from the Greenland to the Labrador Sea, *Geophys. Res. Lett.*, *32*, L10615, doi:10.1029/2005GL022700.

Tanhua, T., A. Biastoch, A. Körtzinger, H. Lüger, C. Böning, and D. W. R. Wallace (2006), Changes of anthropogenic CO₂ and CFCs in the North Atlantic between 1981 and 2004, *Global Biogeochem. Cycle*, *20*, GB4017.

Tanhua, T., A. Körtzinger, K. Friis, D. W. Waugh, and D. W. R. Wallace (2007), An estimate of anthropogenic CO2 inventory from decadal changes in ocean carbon content, *PNAS*, *104*(9), 3037–3042.

Thomas, H., and M. H. England (2002), Different oceanic features of anthropogenic CO₂ and CFCs, *Naturwissenschaften*, *89*, 399–403.

Thomas, H., and V. Ittekkot (2001), Determination of anthropogenic CO₂ in the North Atlantic Ocean using water mass ages and CO₂ equilibrium chemistry, *J. Mar. Syst.*, *27*, 325–336.

Thomas, H., M. England, and V. Ittekkot (2001), An off-line 3D model of anthropogenic CO2 uptake by the oceans, *Geophys. Res. Lett.*, *28*(3), 547–550.

Touratier, F., and C. Goyet (2004), Applying the new TrOCA approach to assess the distribution of anthropogenic CO2 in the Atlantic Ocean, *J. Mar. Syst.*, *46*, 181–197.

Vázquez-Rodríguez, M., F. Touratier, C. Lo Monaco, D. W. Waugh, X. A. Padin, R. G. J. Bellerby, C. Goyet, N. Metzl, A. F. Ríos, and F. F. Pérez (2008), Anthropogenic carbon distributions in the Atlantic Ocean: Data-based estimates from the Arctic to the Antarctic, *Biogeosciences Discuss.*, *5*, 1421–1443.

Vollmer, M. K., and R. F. Weiss (2002), Simultaneous determination of sulfur hexafluoride and three chlorofluorocarbons in water and air, *Mar. Chem.*, *78*(2–3), 137–148.

Walker, S. J., R. F. Weiss, and P. K. Salameh (2000), Reconstructed histories of the annual mean atmospheric mole fractions for the halocarbons CFC-11, CFC-12, CFC-113 and carbon tetrachloride, *J. Geophys. Res.*, *105*(C6), 14,285–14,296.

Wallace, D. W. R. (2001), Ocean measurements and models of carbon sources and sinks, global biogeochemical cycles, *Global Biogeochem. Cycles*, *15*(1), 3–11.

Wallace, D. W. R., and J. R. N. Lazier (1988), Anthropogenic chlorofluoromethanes in newly formed Labrador Sea water, *Nature*, *332*, 61–63.

Warner, M. J., and R. F. Weiss (1985), Solubilities of chlorofluorocarbons 11 and 12 in water and sea water, *Deep Sea Res.*, *32*, 1485–1497.

Watanabe, Y., A. Shimamoto, and T. Ono (2003), Comparison of time-dependent tracer ages in the western North Pacific: Oceanic background levels of SF6, CFC-11. CFC-12 and CFC-113, *J. Oceanogr.*, *59*, 719–729.

Watson, A. J., and J. R. Ledwell (2000), Oceanic tracer release experiments using sulphur hexafluoride, *J. Geophys. Res.*, *105*(C6), 14,325–14,337.

Waugh, D. W., T. M. Hall, and T. W. N. Haine (2003), Relationship among tracer ages, *J. Geophys. Res.*, *108*(C5), 3138, doi:10.1029/2002JC001325.

Waugh, D. W., T. M. Hall, and T. W. N. Haine (2004), Transport times and anthropogenic carbon in the subpolar North Atlantic Ocean, *Deep Sea Res., Part I*, *51*, 1471–1491, doi:10.1016/j.dsr.2004.06.011.

Waugh, D. W., T. M. Hall, B. I. McNeil, R. Key, and R. J. Matear (2006), Anthropogenic CO2 in the Oceans estimated using transit-time distributions, *Tellus, Ser. A and Ser. B*, *58B*, 376–389, doi:10.1111/j.1600-0889.2006.00222.x.

Zhao, J., J. Y. Sheng, R. J. Greatbatch, K. Azetsu-Scott, and E. P. Jones (2006), Simulation of CFCs in the North Atlantic Ocean using an adiabatically corrected ocean circulation model, *J. Geophys. Res.*, *111*, C06027, doi:10.1029/2004JC002814.

T. Tanhua and D. W. R. Wallace, Leibniz-Institut für Meereswissenschaften, Marine Biogeochemie, Düsternbrooker Weg 20, D-24105 Kiel, Germany. (ttanhua@ifm-geomar.de)

D. W. Waugh, Department of Earth and Planetary Sciences, Johns Hopkins University, 3400 North Charles Street, Baltimore, MD 21218, USA.